

Semigeostrophic Invertibility Experiments with TAMEX Data

HUNG-CHI KUO¹ and SHU-WU CHEN¹

(Manuscript received 31 March 1992, in final form 30 April 1993)

ABSTRACT

The balanced atmospheric response to a squall line as a moving heat source is computed. Specifically, we consider the permanent modifications to the large-scale balanced flow (geostrophy) rather than the transient gravity-inertia wave motion. The potential vorticity anomaly, horizontal and vertical wind shears in terms of a dimensionless parameter α and swept-through distance of the squall line are presented. The physical meanings of the parameter α are discussed. Observational cases from mid-latitude, subtropics and tropics are given in terms of the squall line speed and α . This classification is based on the balanced atmospheric response that the squall line induced. Namely, we emphasize the concept of potential vorticity and balanced dynamics to classify the squall lines. The α -c classification will provide a measure of the squall line force in dynamic models. The computed balanced solutions give a reference base to monitor the geostrophic adjustment processes. Moreover, the α -c observations enable us to interpret the model result related to different observational squall lines. The invertibility computations from squall lines during Taiwan Area Mesoscale EXperiment (TAMEX) are shown. The implication of the results and future research are discussed.

1. INTRODUCTION

The semigeostrophic system is a filtered set of equations providing remarkably accurate descriptions of many phenomena which lie beyond description by the quasi-geostrophic equations. Traditionally, the phenomena studied include surface and upper tropospheric fronts, jets and occluding baroclinic waves. The first exploitation of the semigeostrophic system was the two-dimensional frontogenesis studies of Hoskins (1971) and Hoskins and Bretherton (1972). Imposing a horizontal deformation field to force the frontogenesis as in the study made by Hoskins (1972), the semigeostrophic system is able to generate infinite temperature gradient at the surface in less than 12 hours. This is owing to the feedback of geostrophic relative vorticity ζ_g and the ageostrophic secondary circulation in the semigeostrophic system, which is missing in the quasigeostrophic system. By combining the geostrophic momentum

¹ Department of Atmospheric Sciences, National Taiwan University, Taipei, Taiwan, R.O.C.

approximation (Eliassen, 1948) and the geostrophic coordinate transformation (Yudin, 1955), a comprehensive semi-geostrophic theory in three dimensions was worked out by Hoskins (1975) and Hoskins and Draghici (1977). Later frontogenesis studies by Hoskins (1976), Hoskins and West (1979) and Hoskins and Heckley (1981) involved the forcing from a developing baroclinic wave with Eady waves and uniform potential vorticity flows. A study of the energy cascade predicted by the semigeostrophic theory of frontogenesis can be found in Andrews and Hoskins (1978).

In these mid-latitude baroclinic wave and frontogenesis studies with semigeostrophic system, the potential vorticity field is of central attention. The potential vorticity previously has been used as a passive tracer, for example, to trace the entrainment of stratospheric air into the troposphere (Danielsen, 1968). Thus, only the conservation property of Rossby-Ertel potential vorticity has been emphasized. The more recent view has added dynamics to it—the concepts of balance dynamics, invertibility and transformed horizontal coordinates. It provides the simplest way to diagnose or predict balanced dynamics through the use of the Rossby-Ertel potential vorticity on isentropic or entropy surfaces. The acceptance of the modern view is in large part due to the discussion of Hoskins *et al.* (1985), who point out that "PV thinking" can lead to increased insight into such phenomena as the formation of cut-off cyclones and blocking anticyclones, Rossby wave propagation, and baroclinic/barotropic instability.

The semigeostrophic equations in terms of "potential vorticity modeling" involve two main mathematical principles, the conservation of potential pseudo-density (the inverse of potential vorticity) and the principle of invertibility. The conservation of pseudo-density serves as the fundamental prediction equation of the model. The invertibility serves as the diagnostics to obtain the balanced wind and mass fields from the predicted potential pseudo-density. Along the path of "potential vorticity modeling", Schubert *et al.* (1989) studied the balanced atmospheric response to the squall line in mid-latitude by the semigeostrophic model.

In this paper, we study the atmospheric equilibrium (geostrophy) response to squall lines during Taiwan Area Mesoscale Experiment (Kuo and Chen, 1990) with a model similar to that of Schubert *et al.* (1989). We present the semigeostrophic model with the entropy ($c_p \ln(\theta/\theta_0)$) vertical coordinate. We discuss the functional dependence of semigeostrophic solutions with an ideal moving heat source in two dimensions. We reinterpret the α parameter introduced by Schubert *et al.* (1989) and stress the importance of the α parameter and the squall line speed c to classify the squall line. Observational squall lines are presented in terms of α and the squall line speed c .

In section 2 we review the three-dimensional and two-dimensional invertibility principles in semigeostrophic theory with the entropy vertical coordinate. The potential vorticity anomaly and wind shears as a functions of α and swept-through region by the squall line in semigeostrophic theory are given in section 3. Section 3 also contains a classification of squall lines and the balanced response of atmosphere to the squall lines during Taiwan Area Mesoscale EXperiment (TAMEX, Kuo and Chen, 1990). Section 4 gives the concluding remarks.

2. SEMIGEOSTROPHIC THEORY IN THE ENTROPY COORDINATE

2.1 Potential Pseudo-density Equation

We begin with the f -plane system of equations with the geostrophic momentum approximation (Eliassen, 1948; Hoskins, 1975) and proceed with an analysis similar to that of

Schubert *et al.* (1989), but rather than using potential temperature θ as the vertical coordinate, we use the entropy

$$s = c_p \ln\left(\frac{\theta}{\theta_0}\right) = c_p \ln\left(\frac{T}{T_0}\right) - R \ln\left(\frac{p}{p_0}\right) \quad (2.1)$$

as vertical coordinate. Here p is the pressure and T the absolute temperature, which are related to density ρ by the ideal gas law $p = \rho RT$, and the subscript 0 denotes a constant reference value (*e.g.*, that at the bottom of the model). The entropy coordinate provides slightly better resolution in the lower atmosphere and avoids the definition of Exner function II, which has no direct physical significance.

Assuming the flow is frictionless, our system becomes

$$\frac{Du_g}{Dt} - fv + \frac{\partial M}{\partial x} = 0, \quad (2.2)$$

$$\frac{Dv_g}{Dt} + fu + \frac{\partial M}{\partial y} = 0, \quad (2.3)$$

$$\frac{\partial M}{\partial s} = T, \quad (2.4)$$

$$\frac{D\sigma}{Dt} + \sigma\left(\frac{\partial u}{\partial x} + \frac{\partial v}{\partial y} + \frac{\partial \dot{s}}{\partial s}\right) = 0, \quad (2.5)$$

where

$$(u_g, v_g) = \frac{1}{f}\left(-\frac{\partial M}{\partial y}, \frac{\partial M}{\partial x}\right), \quad (2.6)$$

are the components of geostrophic velocity, (u, v) the horizontal components of total velocity, $M = c_p T + \phi$ the Montgomery potential, $\sigma = -\frac{\partial p}{\partial s}$ the pseudo-density, and

$$\frac{D}{Dt} = \frac{\partial}{\partial t} + u \frac{\partial}{\partial x} + v \frac{\partial}{\partial y} + \dot{s} \frac{\partial}{\partial s} \quad (2.7)$$

the total derivative.

The equation for the *isentropic* absolute vorticity can be derived from (2.2) and (2.3). It takes the form

$$\frac{D\zeta}{Dt} + \zeta\left(\frac{\partial u}{\partial x} + \frac{\partial v}{\partial y}\right) - \left(\xi \frac{\partial}{\partial x} + \eta \frac{\partial}{\partial y}\right)\dot{s} = 0, \quad (2.8a)$$

or alternately, the potential vorticity form

$$\frac{\partial}{\partial t}(\sigma q) + \frac{\partial}{\partial x}(u\sigma q - \dot{s}\xi) + \frac{\partial}{\partial y}(v\sigma q - \dot{s}\eta) = 0, \quad (2.8b)$$

where $q = \zeta/\sigma$ is the Rossby-Ertel potential vorticity and where the components of the three dimensional absolute vorticity vector are given by

$$\begin{aligned}\xi &= f \frac{\partial(X, Y)}{\partial(y, s)} = -\frac{\partial v_g}{\partial s} + \frac{1}{f} \frac{\partial(u_g, v_g)}{\partial(y, s)}, \\ \eta &= f \frac{\partial(X, Y)}{\partial(s, x)} = \frac{\partial u_g}{\partial s} + \frac{1}{f} \frac{\partial(u_g, v_g)}{\partial(s, x)}, \\ \zeta &= f \frac{\partial(X, Y)}{\partial(x, y)} = f + \frac{\partial v_g}{\partial x} - \frac{\partial u_g}{\partial y} + \frac{1}{f} \frac{\partial(u_g, v_g)}{\partial(x, y)},\end{aligned}\quad (2.9a)$$

with X and Y defined as

$$(X, Y) = \left(x + \frac{v_g}{f}, y - \frac{u_g}{f} \right). \quad (2.9b)$$

The equivalence of (2.8a) and (2.8b) follows easily from the fact that $\partial\xi/\partial x + \partial\eta/\partial y + \partial\zeta/\partial s = 0$. The significance of (2.8b) is discussed by Haynes and McIntyre (1987), who draw attention to the fact that for the primitive equation in the isentropic coordinate a flux form such as (2.8b) leads directly to the theorem that even with diabatic heating and frictional forces "there can be no net transport of Rossby-Ertel potential vorticity across any isentropic surfaces" and that "potential vorticity can neither be created nor destroyed within a layer bounded by two isentropic surfaces." From (2.8b) we conclude that the primitive equation result of Haynes and McIntyre also holds when we make the geostrophic momentum approximation with entropy as vertical coordinate.

We can eliminate the isentropic divergence between (2.5) and (2.8a) to obtain

$$\frac{D\sigma^*}{Dt} + \frac{\sigma^*}{\zeta} \left(\xi \frac{\partial}{\partial x} + \eta \frac{\partial}{\partial y} + \zeta \frac{\partial}{\partial s} \right) \dot{s} = 0, \quad (2.10)$$

where

$$\sigma^* = \frac{f}{\zeta} \sigma \quad (2.11)$$

is the potential pseudo-density.

To gain a deeper understanding of the physical meaning of the potential pseudo-density, consider a small cylindrical element of fluid spinning cyclonically relative to the earth (i.e., $\zeta > f$); this fluid is bounded on the bottom and top by two entropy surfaces. If the flow is adiabatic, we conclude from (2.10) that σ^* is conserved, so that the pseudo-density σ must decrease as the absolute vorticity ζ decreases, i.e. the pressure difference between the bottom and top isentropic surfaces must decrease as ζ is reduced to f . One can imagine a rearrangement process in which mass moves outward in a divergent fashion without crossing both the bottom and top entropy surfaces, leading to a simultaneous reduction of σ and ζ . Of course, if the fluid element were originally spinning anticyclonically relative to the earth (i.e., $\zeta < f$), the rearrangement would require mass to move inward while σ and ζ simultaneously increased. In either case we can interpret the potential pseudo-density σ^* as

the pseudo-density the fluid element would acquire if ζ were changed to f under a frictionless and adiabatic rearrangement process.

Since ζ can be expressed in terms of u_g and v_g and hence M through geostrophic balance (2.6), and since σ can be expressed in terms of T and hence M through hydrostatic balance (2.4), there exists a second-order partial differential equation relating M and σ^* . This equation, along with its associated boundary conditions, is usually referred to as the invertibility principle. Thus, we have (2.10) as a predictive equation for σ^* and an associated invertibility principle from which we diagnose M from a known σ^* . As we shall see from the simplicity of (2.35), σ^* seems to be a more convenient variable than its inverse, the commonly used potential vorticity. In fact, Schubert *et al.* (1991) show that σ^* is a much better variable than the potential vorticity to dynamically define the tropopause in the tropics.

The D/Dt as is expressed in physical space by (2.7), (2.10) involves advection by the total wind, in which case the predictive equation for σ^* and the invertibility principle do not form a closed system. This is the point at which geostrophic coordinates $(X, Y, S, T) = (x + v_g/f, y - u_g/f, s, t)$ entered. Derivatives in (x, y, s, t) space are related to derivatives in (X, Y, S, T) space by

$$\frac{\partial}{\partial t} = \frac{\partial X}{\partial t} \frac{\partial}{\partial X} + \frac{\partial Y}{\partial t} \frac{\partial}{\partial Y} + \frac{\partial}{\partial T}, \quad (2.12)$$

$$\frac{\partial}{\partial x} = \frac{\partial X}{\partial x} \frac{\partial}{\partial X} + \frac{\partial Y}{\partial x} \frac{\partial}{\partial Y}, \quad (2.13)$$

$$\frac{\partial}{\partial y} = \frac{\partial X}{\partial y} \frac{\partial}{\partial X} + \frac{\partial Y}{\partial y} \frac{\partial}{\partial Y}, \quad (2.14)$$

$$\frac{\partial}{\partial s} = \frac{\partial X}{\partial s} \frac{\partial}{\partial X} + \frac{\partial Y}{\partial s} \frac{\partial}{\partial Y} + \frac{\partial}{\partial S}. \quad (2.15)$$

Inverting (2.13) and (2.14) to obtain

$$\frac{\zeta}{f} \frac{\partial}{\partial X} = \frac{\partial Y}{\partial y} \frac{\partial}{\partial x} - \frac{\partial Y}{\partial x} \frac{\partial}{\partial y}, \quad (2.16)$$

$$\frac{\zeta}{f} \frac{\partial}{\partial Y} = -\frac{\partial X}{\partial y} \frac{\partial}{\partial x} + \frac{\partial X}{\partial x} \frac{\partial}{\partial y}, \quad (2.17)$$

and using (2.16) and (2.17) in (2.15), along with (2.7), we obtain

$$\zeta \frac{\partial}{\partial S} = \xi \frac{\partial}{\partial x} + \eta \frac{\partial}{\partial y} + \zeta \frac{\partial}{\partial s}, \quad (2.18)$$

which shows that $\partial/\partial S$ is the derivative along the vorticity vector and that (X, Y, S, T) are what might be called "vortex coordinates."

To express the geostrophic and hydrostatic equations in (X, Y, S, T) space, it is convenient to introduce the Bernoulli function

$$M^* = M + \frac{1}{2}(u_g^2 + v_g^2). \quad (2.19)$$

Applying (2.15), (2.16) and (2.17) to the Bernoulli function, it can be shown that geostrophic and hydrostatic relations in (X, Y, S, T) take the form

$$(fu_g, fv_g, T) = \left(-\frac{\partial M^*}{\partial Y}, \frac{\partial M^*}{\partial X}, \frac{\partial M^*}{\partial S}\right), \quad (2.20)$$

which are identical to the form taken in (x, y, s, t) .

The transformation relations (2.12)–(2.15) imply that the total derivative given by (2.7) can also be written as

$$\frac{D}{Dt} = \frac{\partial}{\partial T} + \dot{X} \frac{\partial}{\partial X} + \dot{Y} \frac{\partial}{\partial Y} + \dot{s} \frac{\partial}{\partial S}, \quad (2.21)$$

where $\dot{X} = DX/Dt$ and $\dot{Y} = DY/Dt$. In the frictionless atmosphere, it can be easily shown that

$$\dot{X} = u_g, \quad (2.22)$$

$$\dot{Y} = v_g. \quad (2.23)$$

A major advantage of the transformation from (x, y, s, t) space to (X, Y, S, T) space is the change from advection by (u, v) to advection by (\dot{X}, \dot{Y}) , which reduces to advection by (u_g, v_g) in the frictionless case.

With the help of (2.18), the potential pseudo-density equation (2.10) can be simplified as

$$\frac{D\sigma^*}{Dt} + \sigma^* \frac{\partial \dot{s}}{\partial S} = 0. \quad (2.34)$$

Using (2.21) we can write (2.34) in the flux form

$$\frac{\partial \sigma^*}{\partial T} + \frac{\partial}{\partial X}(\dot{X}\sigma^*) + \frac{\partial}{\partial Y}(\dot{Y}\sigma^*) + \frac{\partial}{\partial S}(\dot{s}\sigma^*) = 0, \quad (2.35)$$

which serves as the fundamental predictive equation of the model.

2.2 Invertibility Principle in Two and Three Dimensions

The invertibility principle relates σ^* to M^* . From the definition of σ^* in (2.11) and the definition of isentropic vorticity

$$\frac{f}{\zeta} = \frac{\partial(x, y)}{\partial(X, Y)} = 1 - \frac{1}{f} \left(\frac{\partial v_g}{\partial X} - \frac{\partial u_g}{\partial Y} \right) + \frac{1}{f^2} \frac{\partial(u_g, v_g)}{\partial(X, Y)}, \quad (2.36)$$

we have

$$\frac{\partial(x, y, p)}{\partial(X, Y, S)} + \sigma^* = 0. \quad (2.37)$$

Expressing x and y in terms of u_g and v_g , and then using the equation of state $p = \rho RT$, geostrophic and hydrostatic balances of (2.20), we can write (2.37) as

$$\frac{R}{f^4} \begin{pmatrix} M_{XX}^* - f^2 & M_{XY}^* & M_{XS}^* \\ M_{XY}^* & M_{YY}^* - f^2 & M_{YS}^* \\ \rho M_{XS}^* & \rho M_{YS}^* & (\rho M_S^*)_S \end{pmatrix} + \sigma^* = 0 \quad (2.38a)$$

If the upper boundary is an entropy surface with entropy S_{top} and the temperature T_{top} is specified there (e.g. T is constant for an isothermal top), the upper boundary condition for (2.38a) is simply

$$\frac{\partial M^*}{\partial S} = T_{top} \quad \text{at} \quad S = S_{top}, \quad (2.38b)$$

where $S_{top} = c_p \ln(\theta_{top}/\theta_0)$. Likewise the lower boundary is the isentropic surface with potential temperature $\theta = \theta_0$ and the geopotential is specified there (e.g. $\phi_{bot} = 0$ for a flat surface), then $M = c_p T + \phi_{bot}$ at $S = 0$. Written in terms of M^* , this lower boundary condition becomes

$$M^* - c_p \frac{\partial M^*}{\partial S} - \frac{1}{2f^2} \left(\frac{\partial M^*}{\partial X} \right)^2 - \frac{1}{2f^2} \left(\frac{\partial M^*}{\partial Y} \right)^2 = \phi_{bot} \quad \text{at} \quad S = 0. \quad (2.38c)$$

Together with appropriate lateral boundary conditions, equations (2.35), (2.20) and (2.38) form a closed system for three dimensional invertibility. The computational scheme is as follows: knowing σ^* , solve (2.38) for M^* ; use (2.20) to compute (u_g, v_g) ; use these geostrophic wind winds in (2.35) to predict a new σ^* .

Considering an infinitely long squall line which induces a two-dimensional flow with $\partial/\partial y = \partial/\partial Y = 0$, $u = u_a$ (i.e. $u_g = 0$) and $v = v_g$ (i.e. $v_g = 0$). Equation (2.35) then reduces to

$$\frac{\partial \sigma^*}{\partial T} + \frac{\partial}{\partial S}(\dot{s}\sigma^*) = 0, \quad (2.39)$$

and (2.38) to

$$(f^2 - \frac{\partial^2 M^*}{\partial X^2}) \frac{\partial}{\partial S}(\rho \frac{\partial M^*}{\partial S}) + \rho \left(\frac{\partial^2 M^*}{\partial X \partial S} \right)^2 + f^2 \frac{\sigma^*}{R} = 0. \quad (2.40a)$$

$$\frac{\partial M^*}{\partial S} = T_{top} \quad \text{at} \quad S = S_{top}, \quad (2.40b)$$

$$M^* - c_p \frac{\partial M^*}{\partial S} - \frac{1}{2f^2} \left(\frac{\partial M^*}{\partial X} \right)^2 = \phi_{bot} \quad \text{at} \quad S = 0. \quad (2.40c)$$

Because the geostrophic flow does not advect σ^* in the two-dimensional case, we can now solve (2.39) for σ^* independent of the solution of (2.40).

3. ATMOSPHERIC BALANCED RESPONSE TO SQUALL LINES

3.1 Analytical Solution of Potential Pseudo-density

In our calculation the squall lines will be viewed as a moving heat source. Thus, a moving heat source with a Gaussian shape in X and a mid-tropospheric maximum in two dimension and propagating at constant speed c is considered. The source is

$$\dot{s} = S_0 \exp\left[-\frac{(X - cT)^2}{x_0^2}\right] \sin\left[\frac{\pi S}{S_{top}}\right] \quad (3.1)$$

for $T > 0$, where S_0 is the magnitude which related to a heating rate Q_0 by $S_0 = c_p Q_0 / \theta_0$ and x_0 the e -folding half-width of the heat source.

Substituting (3.1) in (2.39) we obtain

$$\alpha_s e^{\tau^2} \frac{\partial}{\partial \tau} (\sigma^* \sin Z) + \sin Z \frac{\partial}{\partial Z} (\sigma^* \sin Z) = 0, \quad (3.2)$$

where $Z = \pi S / S_{top}$ and $\tau = (cT - X) / X_0$. The dimensionless parameter

$$\alpha_s = \frac{S_{top}/(\pi S_0)}{X_0/c}, \quad (3.3)$$

which is identical to the α introduced by Schubert *et al.* (1989) within the accuracy of $O((S/c_p)^2)$. To unify the symbol with Schubert *et al.* (1989), we will use α from now own. According to (3.2) the quantity $\sigma^* \sin Z$ is constant along each characteristic curve determined from $d\tau / (\alpha e^{\tau^2}) = dZ / (\sin Z)$. By integration of this characteristic equation we can show that the characteristic through the point (X, Z, T) approaches (in the far field) the level

$$Z_0(X, Z, T) = 2 \tan^{-1} \left(e^{-\beta(X, T)} \tan \frac{Z}{2} \right), \quad (3.4)$$

where

$$\beta(X, T) = \frac{\sqrt{\pi}}{2\alpha} \left[\operatorname{erf}\left(\frac{cT - X}{X_0}\right) + \operatorname{erf}\left(\frac{X}{X_0}\right) \right]. \quad (3.5)$$

Let us assume that $X \rightarrow \pm\infty$, σ^* approaches the constant σ_0 . Since $\sigma^* \sin Z$ is constant along each characteristic, we can write the solution of (2.39) as

$$\sigma^*(X, Z, T) = \sigma_0 \frac{\sin Z_0(X, Z, T)}{\sin Z}. \quad (3.6a)$$

Although (3.6a) is indeterminate at the top and bottom boundaries, use of L'Hopital's rule yields

$$\sigma^*(X, Z, T) = \sigma_0 \begin{cases} e^{\beta(X, T)} & Z = \pi \\ e^{-\beta(X, T)} & Z = 0. \end{cases} \quad (3.6b)$$

In summary, (3.6) along with the auxiliary relations (3.4) and (3.5) give the analytic solution of (2.39) with the specified heating (3.1). With the known α and c , we then have $\sigma^*(X, S, T)$. Similar derivation was presented in Schubert *et al.* (1989).

3.2 Importance of α Parameter and Squall Line Speed c

Schubert *et al.* (1989) interpreted α as the ratio of the convective overturning time to the squall line passage time of an air parcel entering the squall line. In general, α is small for heavily raining, wide, slowly moving squall lines while it is large for weakly raining, narrow, fast moving squall lines. To interpret α differently, we write $\alpha = (S_{top}c)/(\pi S_0 X_0)$ which is the ratio of time rate of area (mass) in (X, S) space span by the moving squall line to the time rate of entropy change by the squall line heat source. Since the potential vorticity is the mass inside X and S , α may also be interpreted as the inverse of the potential vorticity production or reduction rate for the region that the squall line swept through. Thus, the above interpretations link potential vorticity anomaly to α . Together with the invertibility equation (2.40), we have the squall line heat source as a physical analog of the static electric field. The squall line heat source charges the air parcel that flows into it with potential vorticity. The balanced flow induced by the potential vorticity anomaly corresponds to the electrical field intensity, the potential vorticity corresponds to charge density and the Bernoulli function M^* corresponds to the electrical potential. The only difference lies in the linear elliptical (poisson) equation involved in a static electrical field calculation while the invertibility calculation in (2.40) is nonlinear.

To substantiate the idea that α is the inverse of the potential vorticity production or reduction rate for the region swept-through by the squall line, we have examined the extreme PV anomaly produced by the heat source (3.1) in the semigeostrophic solution. Our calculation indicates that the extreme PV anomaly value produced by a moving heat source (squall line) is indeed a function of α only. It is not a function of squall line speed c or time. The maximum q/f (normalized potential vorticity) as a function of α in the lower atmosphere and the minimum q/f as a function of α in the upper atmosphere are presented in Figure 1. In addition to a fixed α , we have found that the balanced response of the atmosphere

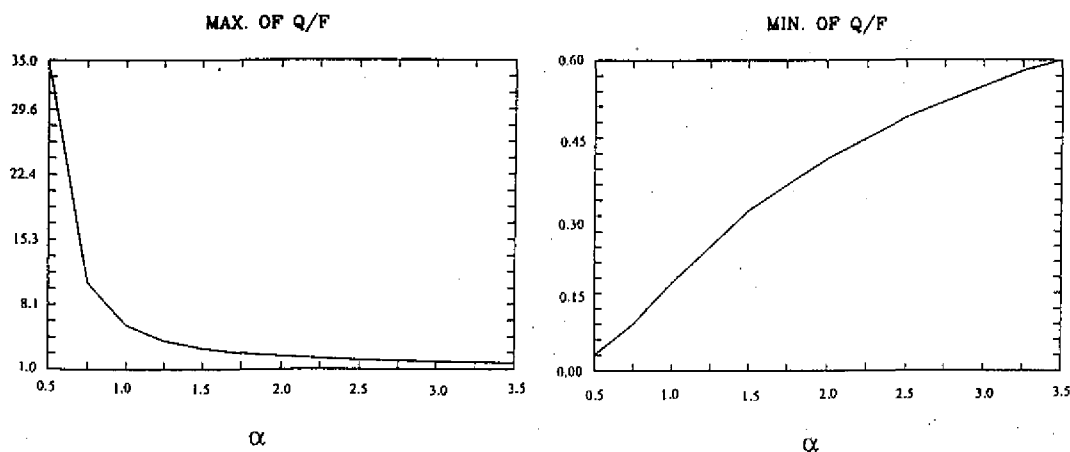


Fig. 1. The maximum normalized q/f as a function of α in the lower atmosphere and the minimum normalized q/f as a function of α in the upper atmosphere.

depends only on the swept-through distance of the heat source. The permanent modifications to the large-scale balanced flow by the moving heat source depend on the PV anomaly and the size of the anomaly region. For example, the response of $c = 5 \text{ m/s}$ at hour 10 is the same as the response of $c = 10 \text{ m/s}$ at hour 5 for a fixed α . Figures 2 and 3 give the maximum horizontal wind shear across the PV anomaly in the upper and lower atmosphere. Figure 4 presents the maximum vertical wind shear (holding X fixed) in the unit of $\text{ms}^{-1} \text{hPa}^{-1}$. The ordinate in these figures is the swept- through distance of heat source. Thus the figures give a quantitative measure in either the balanced wind shear as a function of α and c at a fixed time or the time evolution of balanced wind shear for a fixed α . There is an increase in both upper and lower atmospheric horizontal wind shears as the swept-through distance and α decrease. On the other hand, the vertical wind shear increases as α decreases and the swept-through distance increases.

Since the balanced responses are functions of α and swept-through distance only, we can then use α , squall line speed c and Figures 2, 3 and 4 to classify the squall lines. This classification is based on the balanced atmospheric response induced by the squall line. Thus, the concept of potential vorticity and balanced dynamics are used. Table 1 gives the α values during the TAMEX and squall lines observed during the January–March period of 1988. Because all of the squall lines in TAMEX are over the Taiwan Strait, the heating rate Q_0 (thus S_0) in these cases are evaluated based on the total precipitation and assuming that the vertical heating profile takes the form of a half sine wave as in (3.1). This half sine wave profile is an idealization for a typical cumulus apparent heat source. The total precipitation is calculated from the radar data (Chen and Chou, 1993). The X_0 and c are tabulated from the GMS satellite picture as well as from radar data. Observational squall lines from COPT81 (Roux, 1988), GATE (Houze, 1977), TAMEX (Chen and Chou, 1993) and mid-latitude

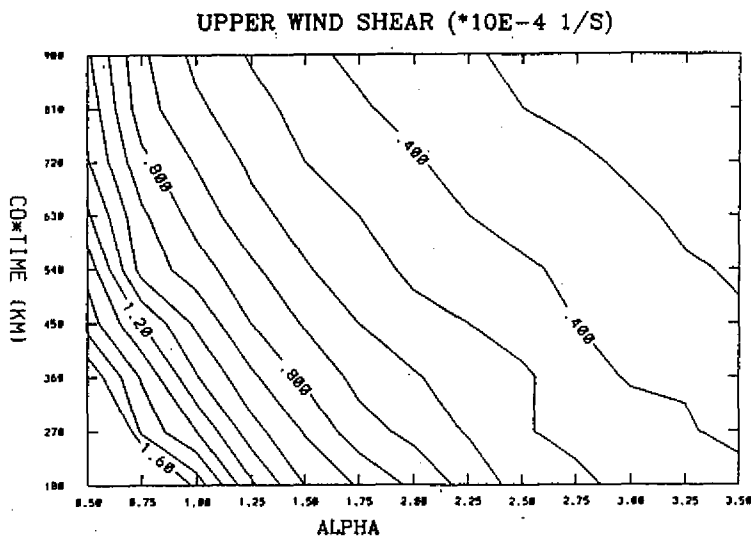


Fig. 2. The maximum horizontal wind shear across the PV anomaly in the upper atmosphere as a function of the swept-through distance of heat source (ordinate) and α (abscissa).

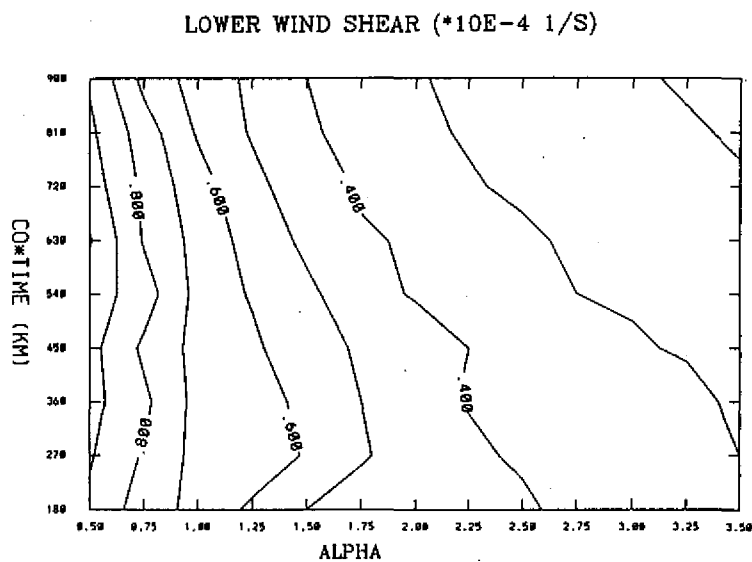


Fig. 3. The maximum horizontal wind shear across the PV anomaly in the lower atmosphere as a function of the swept-through distance of heat source (ordinate) and α (abscissa).

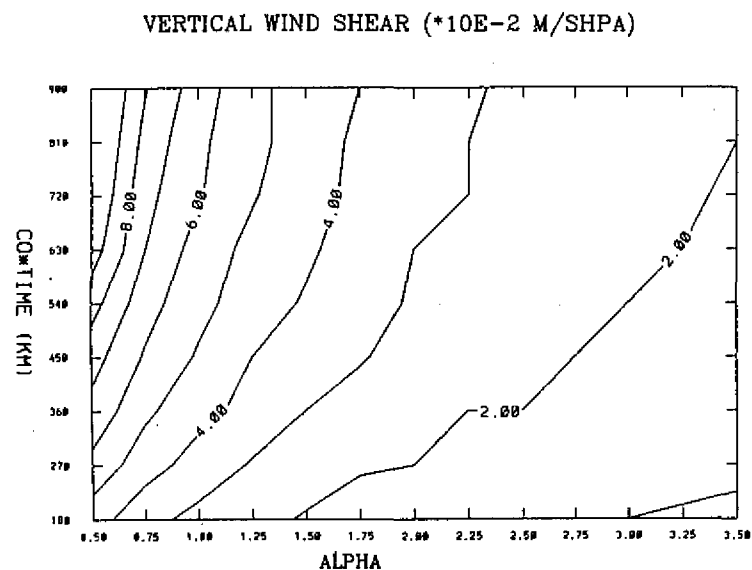


Fig. 4. The maximum vertical wind shear (holding X fixed) in the unit of $m s^{-1} hPa^{-1}$ as a function of the swept-through distance of heat source (ordinate) and α (abscissa).

Oklahoma (Schubert *et al.* 1989 and Hertenstein and Schubert, 1991) are given in terms of squall line speed c and α in Figure 5. Also included are two cases of the squall lines observed near northern Taiwan on March 4, 1988. The much larger α cases in Table 1 are omitted for plotting clarity.

The case studied by Schubert *et al.* (1989) is the typical Oklahoma squall line of which $\alpha = 2.3$. The TAMEX cases are different as compared to mid-latitude Oklahoma cases in that α and c in TAMEX are smaller. This is due to the high humidity environment in the TAMEX cases as compared to the much drier mid-latitude Oklahoma cases. The very humid background probably leads to a stronger precipitation heating rate (thus a smaller α) and a lack of cold air behind the squall line (thus the slower moving speed). The March 4 squall lines have much larger α and smaller c than the TAMEX cases. These squall lines had less rain than the TAMEX cases. The COPT81 and GATE cases share similar α value as the TAMEX cases and possess a faster moving speed. According to Figures 2, 3 and 4, the TAMEX squall lines tend to produce larger balanced horizontal wind shears in the upper atmosphere than the COPT81 and the GATE squall lines. On the other hand, the COPT81 and the GATE squall lines have twice as much balanced vertical wind shears.

Table 1. The width, length, propagation speed, heating rate and computed α during TAMEX. Also included are the squall lines observed during January–March period 1988 over the ocean near the northern part of Taiwan.

parameter case	X. width (Km)	length (Km)	C (Km/hr)	Q. (K/hr)	α
I O P 2	42	280	59.4	10.0	1.78
S O P	40	270	37.8	10.0	1.20
I O P 3 B	46	300	34.2	10.0	0.95
I O P 6	30	210	30.6	10.0	1.29
I O P 8	25	200	28.8	10.0	1.46
I O P 1 3	30	220	18	10.0	0.76
1988.1.31	12.5	150	74.9	3.4	11.17
1988.1.31	7.5	100	58.3	3.4	14.50
1988.1.31	10	75	93.6	3.4	17.45
1988.1.31	10	100	32.0	3.4	11.95
1988.3.25	10	140	14.0	3.4	2.62
1988.3.04	15	200	13.7	3.4	1.70
1988.3.04	15	120	8.6	3.4	1.08

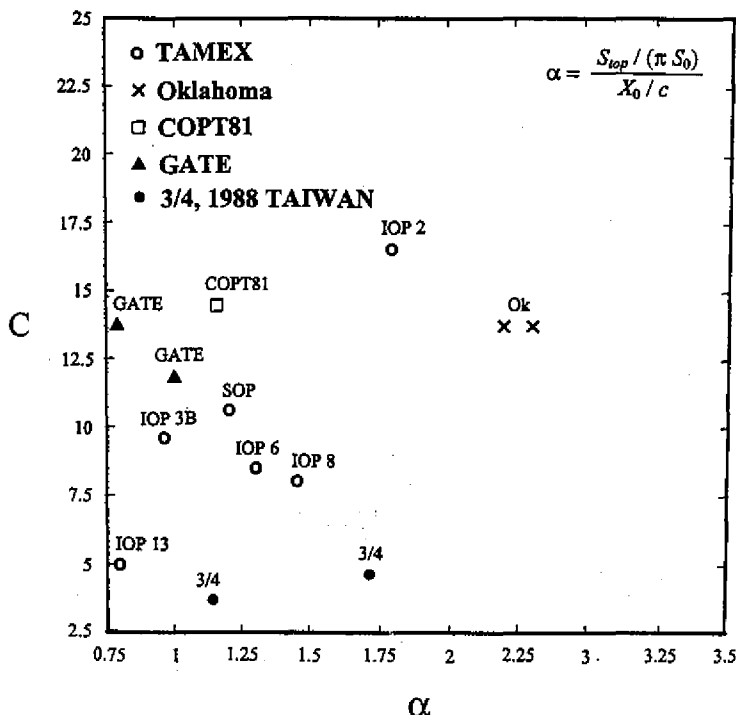


Fig. 5. Observational squall lines from COPT81 (Roux, 1988), GATE (Houze, 1977), TAMEX (Chen and Chou, 1993) and mid-latitude Oklahoma (Schubert *et al.* 1989 and Hertenstein and Schubert, 1991) as a function of squall line speed $c(ms^{-1})$ and parameter α .

3.3 Invertibility Calculation with TAMEX Squall Lines

Figures 6–11 give results of non-dimensionalized q , the geostrophic flow and the disturbed pressure at $T = 16hr$ with the c and α of the TAMEX cases given in Table 1. The θ is used in the plotting rather than the entropy S . It is interesting to note that the induced geostrophic balanced flow covers a region greater than the region swept through by the squall line. Behind the squall line there is a decrease in σ (stabilization) in the lower troposphere and an increase in σ (destabilization) in the upper troposphere. This is a reflection of the mutual adjustment between the wind and mass fields. This adjustment happens in such a way that $q = \zeta/\sigma$ is large in the lower part and small in the upper part. We have larger ζ and smaller σ for large q and the opposite for small q . Whether this upper destabilization will provide a favorable background for the upper stratiform precipitation is beyond the scope of our semigeostrophic model. Although the solutions have similar structure as compared to the mid-latitude case studied by Schubert *et al.* (1989), the TAMEX cases (with the exception of IOP2 case) apparently possess a much stronger wind shear. It is possible that these large horizontal wind shears cause a barotropic type of instability.

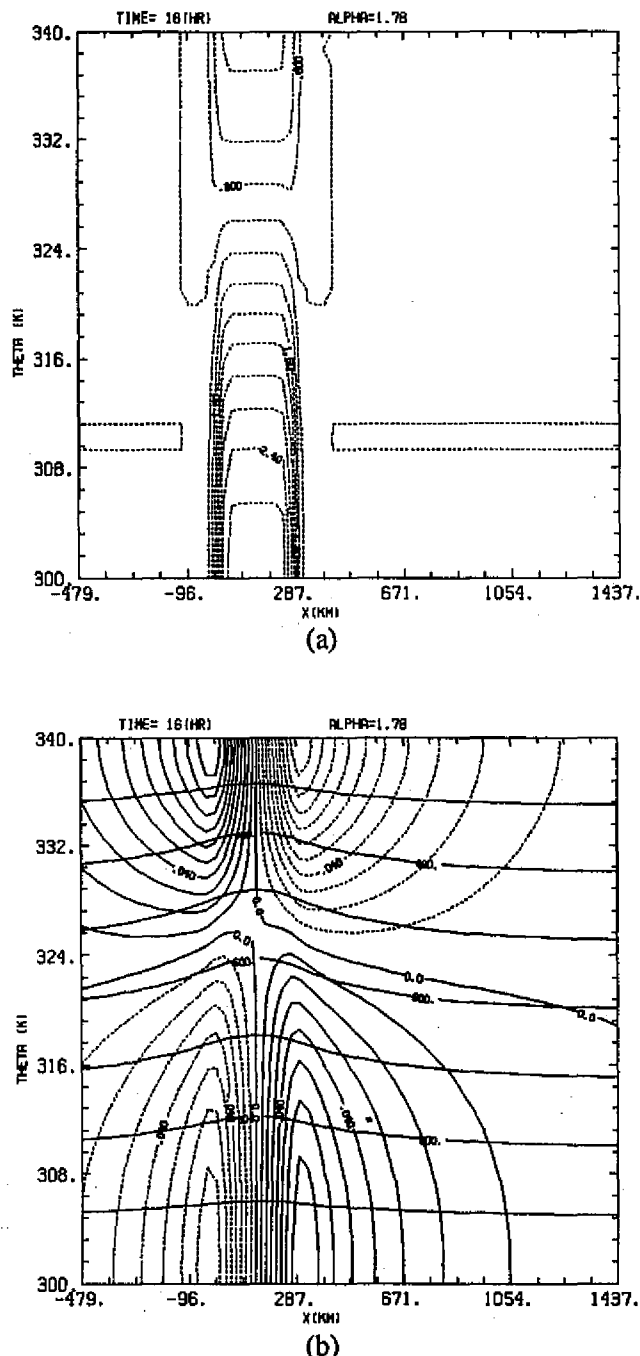


Fig. 6. The normalized potential vorticity q/f (a), the geostrophic flow and the disturbed pressure (b) at $T = 16\text{hr}$ in IOP2 case of TAMEX. The geostrophic wind speed is scaled by 100.0. The wind interval is 1ms^{-1} . The dashed lines are out of page and solid lines are into the page. The disturbed pressure is in the unit of hPa . The corresponding α , c and Q_0 can be found in table 1.

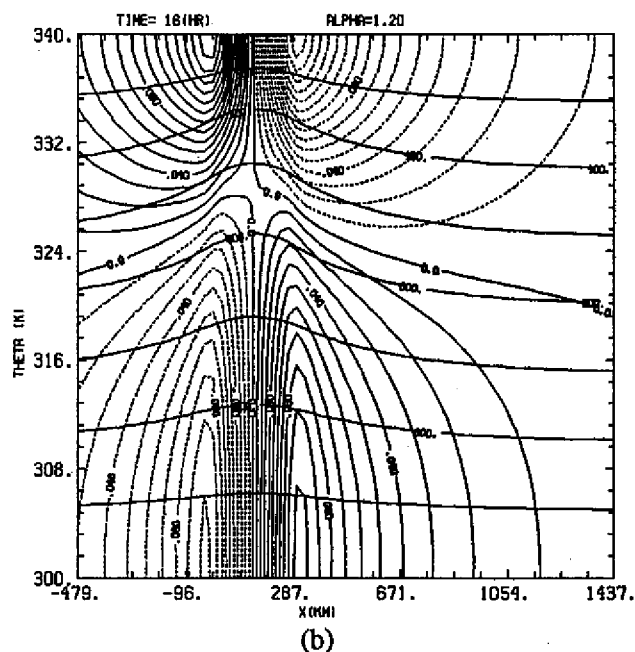
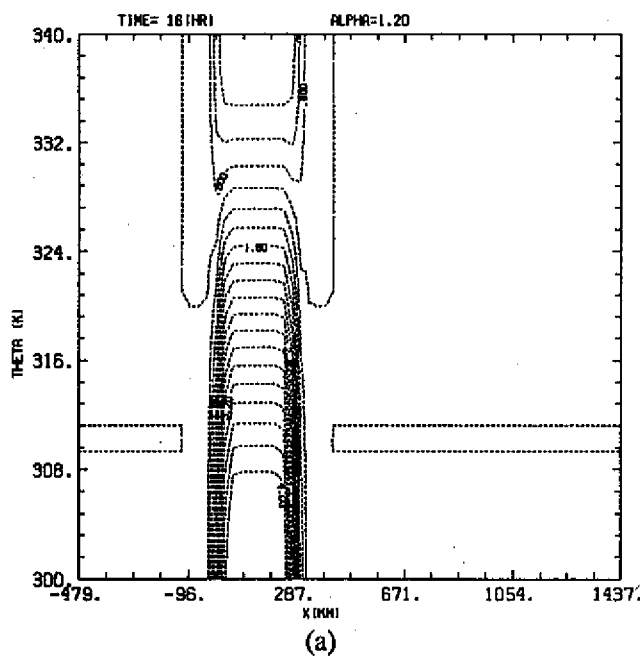


Fig. 7. Same as Fig. 6 except for the SOP case of TAMEX.

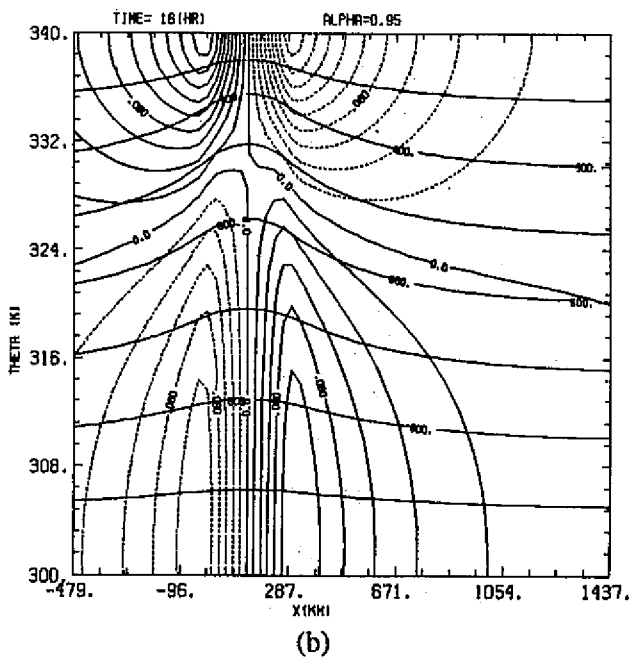
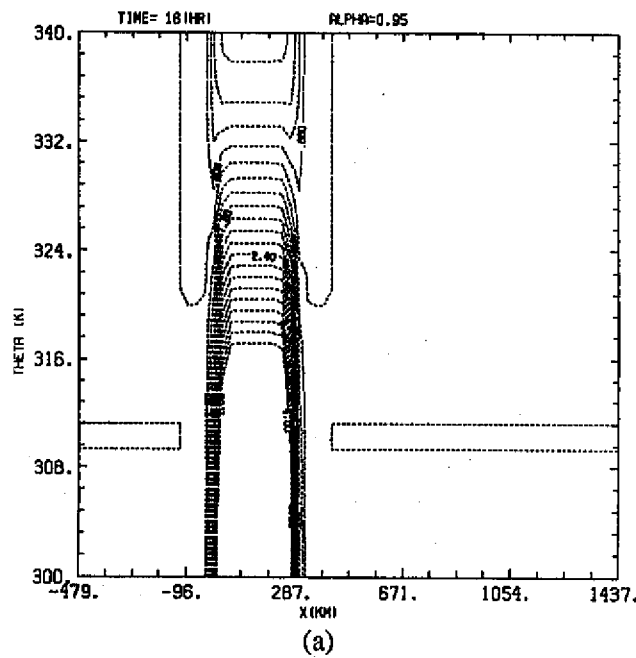


Fig. 8. Same as Fig. 6 except for the IOP3B case of TAMEX.

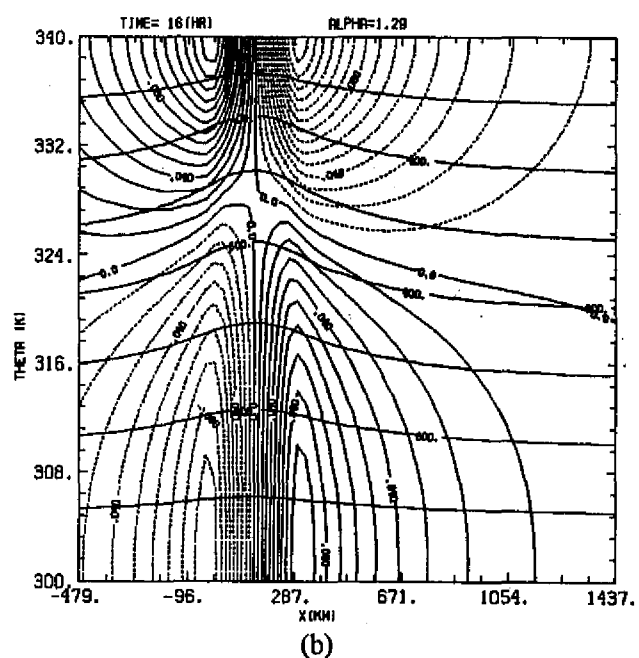
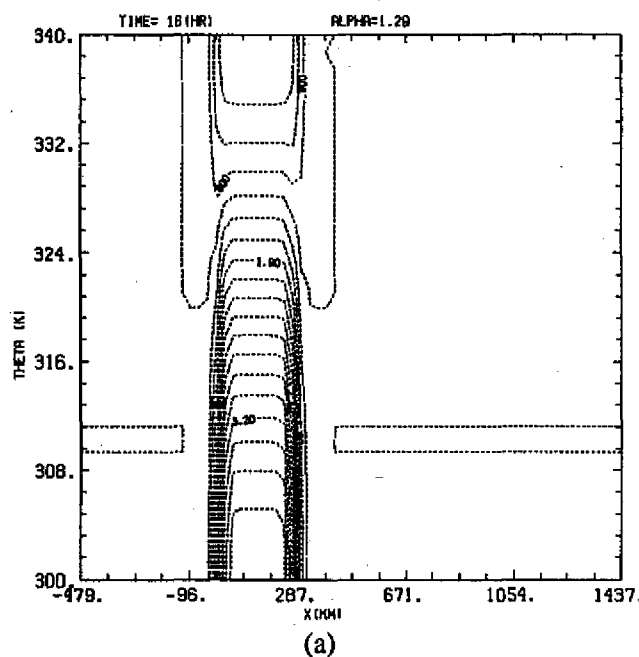


Fig. 9. Same as Fig. 6 except for the IOP6 case of TAMEX.

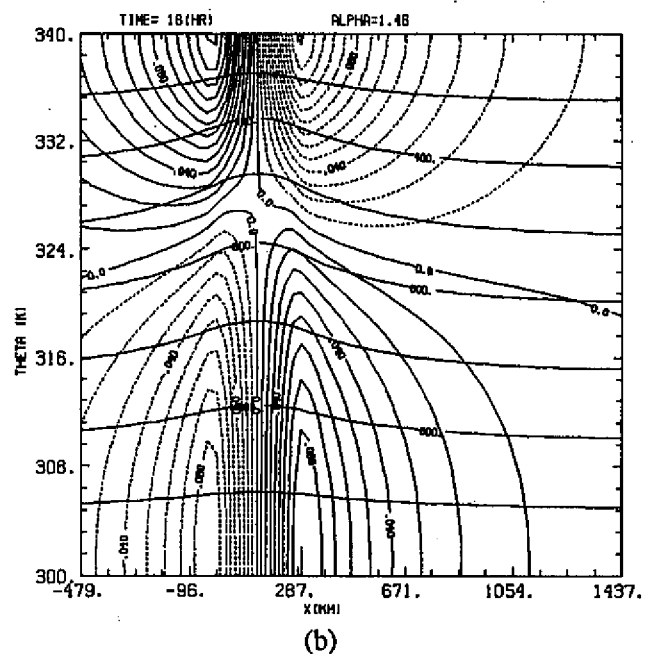
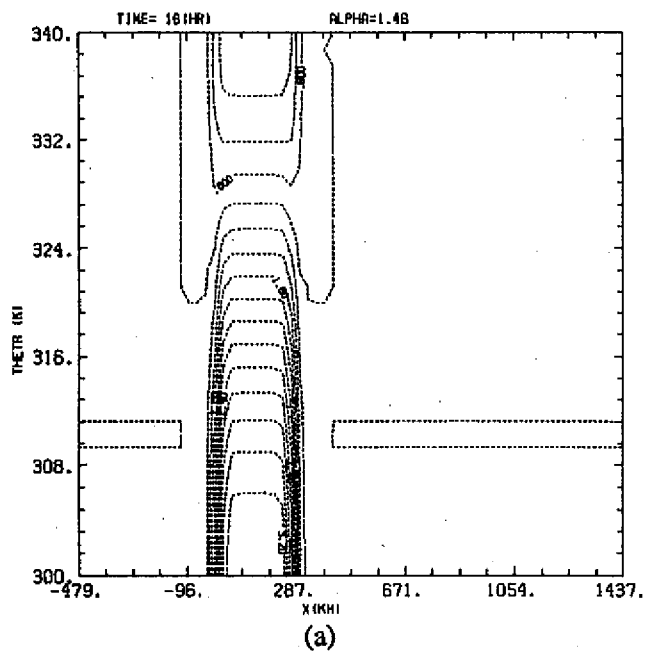


Fig. 10. Same as Fig. 6 except for the IOP8 case of TAMEX.

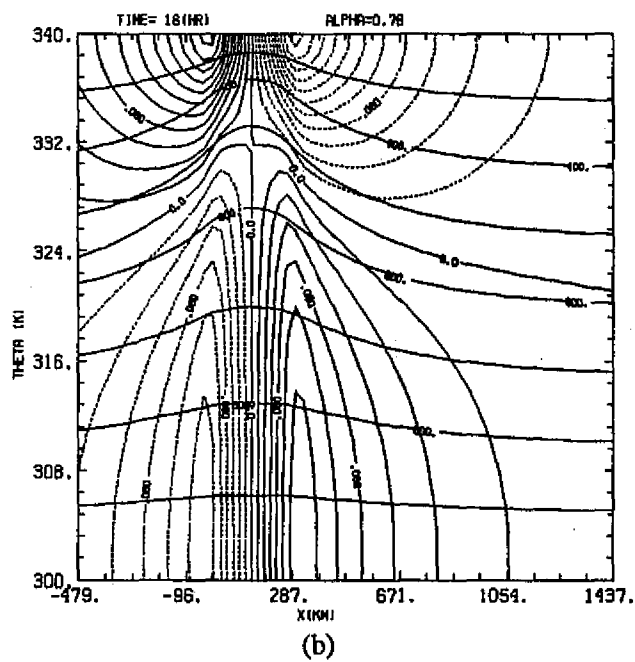
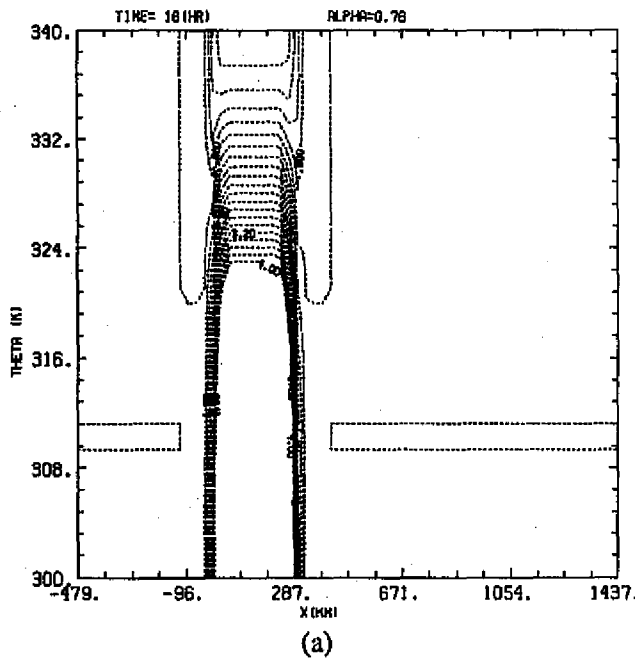


Fig. 11. Same as Fig. 6 except for the IOP13 case of TAMEX.

4. CONCLUDING REMARKS

Our calculations are a direct application of semigeostrophic invertibility solution of Schubert *et al.* (1989) with TAMEX data. We have presented the semigeostrophic model in entropy coordinate and the balanced responses from squall lines during Taiwan Area Mesoscale Experiment (TAMEX). We have discussed the physical meaning of potential pseudo-density and α parameter. We have also discussed the functional dependence of the Schubert *et al.* (1989) solution. Namely, the balanced atmospheric responses to the squall lines depends only on the potential vorticity anomaly and anomaly size. The potential vorticity anomaly is a function of α only while the anomaly size is related to the region swept through by the squall line. The potential vorticity anomaly, horizontal and vertical wind shears as a function of the dimensionless parameter α and the swept-through distance of the squall line are given. Observational cases from COPT81, TAMEX, GATE and mid-latitude are given in terms of squall line speed c and the α parameter. The TAMEX cases are different as compared to mid-latitude Oklahoma cases in that α and c are smaller. The GATE, COPT81 cases share similar α value as the TAMEX cases and possess a faster moving speed. The α - c classifications of the squall lines are based on their contributions to balanced atmospheric responses. We emphasize the concept of using potential vorticity and balanced dynamics to classify the squall lines. The α and c will provide a measure of the squall line force in dynamic models. The computed balanced solutions provide a reference base to monitor the geostrophic adjustment processes in primitive equation models. Moreover, the α - c observations help us interpret the model result related to different observational squall lines. We are currently trying to construct the α - c climatology of squall lines around Taiwan in different seasons.

There are several ways to extend the research presented here. A natural extension is the semi-geostrophic β plane theory as proposed by Magnusdottir and Schubert (1990). In addition, the atmospheric response is very sensitive to the vertical heating profile of the squall line. The heating profile has yet to be determined from observations. Also, latent heat from the stratiform region has not been considered at all in this study. We need to incorporate this heating in our definition of α .

Raymond and Jiang (1991) discuss the possible relationship of potential vorticity anomaly and the long-lived storm. To look into this effect, we need not only good numerical advection schemes, but also fast three-dimensional invertibility solvers. To consider the effect of intersection of entropy surface with a lower boundary, the "massless" layer approach as proposed by Hoskins *et al.* (1985) needs also to be considered. These pose serious challenges for "IPV modeling". In addition to the numerical difficulty in developing the fast elliptical solvers for the invertibility principle, the advection of potential vorticity requires efficient and accurate schemes. Namely, one must cope with sharp gradient of potential vorticity and guarantee the positive definiteness of potential vorticity. In our paper, the advective part of computation is bypassed by the analytical method. In a realistic physical situation that potential vorticity anomaly may be moved by large scale flow and trigger a new convection. A fast invertibility three-dimensional solver has been developed by Fulton and Taft (1991). We are currently testing the positive definiteness advection schemes proposed by Hsu and Arakawa (1990) and Smolarkiewicz (1983).

Finally, we note that the latent heat release associated with the squall line produced a reverse gradient of potential vorticity on a isentropic surface. This barotropic/baroclinic instability deserves more attention. For most cases in TAMEX with α less than 1, squall

line heating is distributed in a small region. The relevance of the instabilities to the actual weather needs to be investigated. The stability analysis of the balanced wind shear is the starting point for future studies.

Acknowledgments The author would like to extend thanks to Professor Scott Fulton for providing the package of multigrid routine, to Professor George Chen for providing TAMEX data and to Professors Richard Johnson, Wayne Schubert and Ben Jong-Dao Jou for helpful discussions. This work was supported by the Grant NSC 80-0202-M002-07 and 81-0202-M002-07 from the National Research Council of Taiwan. The computations were performed at Convex C120 at Department of Atmospheric Sciences in National Taiwan University.

REFERENCES

- Andrews, D. G., and B. J. Hoskins, 1978: Energy spectra predicted by semi-geostrophic theories of frontogenesis. *J. Atmos. Sci.*, 35, 509-512.
- Chen, G. T.-J. and H.-C. Chou, 1993: On the general characteristics of squall lines observed in TAMEX. Accepted in *Mon. Wea. Rev.*.
- Danielsen, E. F., 1968: Stratospheric-tropospheric exchange based on radioactivity and potential vorticity. *J. Atmos. Sci.*, 25, 502-518.
- Eliassen A., 1948: The quasi-static equations of motion. *Geofys. Publ.*, 17, No. 3.
- Fulton, S. R., and R. K. Taft, 1991: Multigrid solvers for the three-dimensional semi-geostrophic equations. Proceeding 9th Conf. on Numerical Weather Prediction., Amer. Meteor. Soc., Denver, 309-312.
- Haynes, P. H., and M. E. McIntyre, 1987: On the evolution of vorticity and potential vorticity in the presence of diabatic heating and frictional or other forces. *J. Atmos. Sci.*, 44, 828-841.
- Hertenstein, R. F. A., and W. H. Schubert, 1991: Potential vorticity anomalies associated with squall lines. *Mon. Wea. Rev.*, 119, 1663-1672.
- Hoskins, B. J., 1971: Atmospheric frontogenesis: some solution. *Quart. J. Roy. Meteor. Soc.*, 97, 139-153.
- Hoskins, B. J., and F. P. Bretherton, 1972: Atmospheric frontogenesis Models: Mathematical formulation and solution. *J. Atmos. Sci.*, 29, 11-37.
- Hoskins, B. J., 1972: Non-Boussinesq effects and further development in a model of upper tropospheric frontogenesis. *Quart. J. Roy. Meteor. Soc.*, 98, 532-541.
- Hoskins, B. J., 1975: The geostrophic momentum approximation and the semi-geostrophic equations. *J. Atmos. Sci.*, 32, 232-242.
- Hoskins, B. J., 1976: Baroclinic waves and frontogenesis . Part I: Introduction and Eady waves. *Quart. J. Roy. Meteor. Soc.*, 102, 103-122.
- Hoskins, B. J., and I. Draghici, 1977: The forcing of ageostrophic motion according to the semi-geostrophic equations and in an isentropic coordinate model. *J. Atmos. Sci.*, 32, No. 12.

- Hoskins, B. J., and N. V. West, 1979: Baroclinic waves and frontogenesis. Part II: Uniform potential vorticity jet flows-cold and warm fronts. *J. Atmos. Sci.*, **36**, 1663-1680.
- Hoskins, B. J. and W. A. Heckley, 1981: Cold and warm fronts in baroclinic waves. *Quart. J. Roy. Meteor. Soc.*, **107**, 79-90.
- Hoskins, B. J., M. E. McIntyre, and A. W. Robertson, 1985: On the use and significance of isentropic potential vorticity maps. *Quart. J. Roy. Meteor. Soc.*, **111**, 877-946.
- Houze, R. A., 1977: Structure and dynamics of a tropical squall-line system. *Mon. Wea. Rev.*, **105**, 1540-1567.
- Hsu, Y.-J., and A. Arakawa, 1990: Numerical modeling of the atmosphere with an isentropic vertical coordinate. *Mon. Wea. Rev.*, **118**, 1933-1959.
- Kuo, Y.-H. and G. T.-J. Chen, 1990: The Taiwan Area Mesoscale Experiment (TAMEX): an overview. *Bull. Amer. Meteor. Soc.*, **71**, 488-503.
- Magnusdottir, G., and W. H. Schubert, 1990: The generalization of semi-geostrophic theory to the β -plane. *J. Atmos. Sci.*, **47**, 1714-1720.
- Raymond, D. J., and H. Jiang, 1990: A theory for long-lived mesoscale convective systems. *J. Atmos. Sci.*, **47**, 3067-3077.
- Roux, F., 1988: The west African squall line observed on 23 June 1981 during COPT 81: kinematics and thermodynamics of the convective region. *J. Atmos. Sci.*, **45**, 406-426.
- Schubert, W. H., P. E. Ciesielski, D. E. Stevens and H.-C. Kuo, 1991: Potential vorticity modeling of the ITCZ and the Hadley circulation. *J. Atmos. Sci.*, **48**, 1493-1509.
- Schubert, W. H., S. R. Fulton, and R. F. A. Hertenstein, 1989: Balanced atmospheric response to squall lines. *J. Atmos. Sci.*, **46**, 2478-2483.
- Smolarkiewicz, P. K., 1983: A simple positive definite advection scheme with small implicit diffusion. *Mon. Wea. Rev.*, **111**, 479-486.
- Yudin, M. I., 1955: Invariant quantities in large-scale atmospheric processes. *Tr. Glav. Geofiz. Observ.*, **55**, 3-12.